Spectroscopy on Individual Light-Harvesting 1 Complexes of *Rhodopseudomonas acidophila*

Martijn Ketelaars,* Clemens Hofmann,† Jürgen Köhler,‡ Tina D. Howard,§ Richard J. Cogdell,§ Jan Schmidt,¶ and Thijs J. Aartsma*

*Department of Biophysics, ¶Centre for the Study of Excited States of Molecules, Huygens Laboratory, Leiden University, 2300 RA Leiden, The Netherlands; †Ludwig-Maximilians-Universität München, Department of Physics and CeNS, Photonics and Optoelectronics Group, 80799 München, Germany; ‡Experimental Physics IV and BZMB, University of Bayreuth, 95440 Bayreuth, Germany; and §Division of Biochemistry and Molecular Biology, Department of Chemistry, University of Glasgow, Glasgow G12 8QQ, United Kingdom

ABSTRACT In this paper the fluorescence-excitation spectra of individual LH1-RC complexes (*Rhodopseudomonas acidophila*) at 1.2 K are presented. All spectra show a limited number of broad bands with a characteristic polarization behavior, indicating that the excitations are delocalized over a large number of pigments. A significant variation in the number of bands, their bandwidths, and polarization behavior is observed. Only 30% of the spectra carry a clear signature of delocalized excited states of a circular structure of the pigments. The large spectral variety suggests that besides site heterogeneity also structural heterogeneity determines the optical spectrum of the individual LH1-RC complexes. Further research should reveal if such heterogeneity is a native property of the complex or induced during the experimental procedures.

INTRODUCTION

The progress made in high-resolution structural studies of light-harvesting complexes of purple bacteria, i.e., the light-harvesting 1 (LH1), light-harvesting 2 (LH2), and B800-820 (LH3) complexes (McDermott et al., 1995; Karrasch et al., 1995; Koepke et al., 1996; Hu et al., 1997; Walz et al., 1998; McLuskey et al., 2001), has strongly stimulated experimental and theoretical investigations to understand the efficient energy transfer in these antenna systems. Especially the correlation between the spatial organization of these pigment-protein complexes and their function is of great interest.

By now it has been established that the spatial structure of photosynthetic complexes, in particular the mutual orientation of the pigments, determine to a large extent their spectroscopic features and excited-state dynamics (van Amerongen et al., 2000). This applies in particular to light-harvesting systems like LH2 and LH1, because the intermolecular interactions of their pigments are relatively strong, they contain few inequivalent binding sites, and their symmetry is very high. All these factors contribute to the consensus that in these systems collective excitations, or Frenkel excitons, play an important role in the excited-state properties and the mechanism of energy transfer. Such excitons arise from the interactions between the optical transition-dipole moments of individual pigment molecules. The size of these interactions can be calculated from the spatial structure of the pigment-protein complex. Thus, the spectroscopic data can provide information about the structural arrangement of the LH complexes.

Currently, two prevailing views exist in the literature to describe the spectroscopic features of the LH1 system. Both views are based on the assumption that LH1 is a closed-ring structure equivalent to LH2. In the first view, the LH1 ring is considered to be a ring of interacting dimers (van Mourik et al., 1992; Visser et al., 1995; Bradforth et al., 1995; Jimenez et al., 1997; van Amerongen et al., 2000), where the dimer corresponds to the two interacting pigments of an $\alpha\beta$-subunit. The interaction within this dimer (intradimer) is considered to be much stronger than the interaction between different dimers (interdimer). Any phase relation between excitations on different dimers is rapidly destroyed, either dynamically due to the coupling to vibrations or phonons or as a consequence of the interference of the pure eigenstates due to site heterogeneity (van Amerongen et al., 2000). This site heterogeneity is caused by the fact that each bacteriochlorophyll *a* (BChl *a*) molecule has a slightly different protein environment due to local disorder and therefore absorbs at a slightly different energy. Usually it is assumed that this excited-state energy varies from one molecule to the other within a Gaussian distribution (Sundström and van Grondelle, 1995). At low temperature it is believed that the site heterogeneity is the dominant factor in the destruction of the phase relation between the excitations on the different dimers. In the alternative view the interaction between the dimers is considered to be of the same size as the intradimer interaction and the excitation is delocalized over a substantial part of the ring. Experimental evidence to support this model was found in hole-burning experiments (Reddy et al., 1992; Wu et al., 1998) and from an estimate of the absorption cross-section of the major transition in LH1 (Novoderezhkin and Razjivin, 1995).

Submitted February 13, 2002 and accepted for publication May 8, 2002.

Address reprint requests to Jürgen Köhler, Experimental Physics IV and BZMB, University of Bayreuth, 95440 Bayreuth, Germany. Tel.: 49-921-554001; Fax: 49-921-554002; E-mail: juergen.koehler@uni-bayreuth.de.

0006-3495/02/09/1701/15 $2.00

Recently we succeeded in observing the fluorescence-excitation spectra of individual LH2 complexes of *Rhodopseudomonas* (*Rps.*) *acidophila* at low temperature (van Oijen et al., 1998). These single-molecule experiments provided direct information about the parameters determining the electronic structure of LH2. The contention is that these parameters are equally important for the description of the properties of LH2 at room temperature in detergent solution as well as in vivo. In particular the spectra observed for the B800 pigment pool of LH2 provided for the first time a direct and detailed insight in the electronic structure of this part of the complex. Among the B800 pigments the intermolecular interaction is smaller than the site heterogeneity and the electronically-excited states are expected to be strongly localized on the individual BChl *a* molecules. The polarization dependence of the observed narrow lines ~800 nm confirmed this contention and is in agreement with the circular arrangement of the BChl *a* molecules. In addition, the contributions of intra- and intercomplex site heterogeneity to the spectral distribution of the optical transitions could be ascertained (van Oijen et al., 2000).

In contrast, the spectra associated with the B850 pigment pool showed completely different characteristics with regard to the number of bands and their widths (van Oijen et al., 1999a; Ketelaars et al., 2001). The spectra were dominated by two broad absorption bands ~860 nm, which in all cases were orthogonally polarized within the accuracy of the measurements. These bands were assigned to the two lowest degenerate states of a circular exciton denoted by their quantum number $k^{\mathrm{circ}} = \pm 1$. The lifting of the degeneracy was attributed to site heterogeneity as well as a reduced symmetry possibly due to a small structural deformation of the circular aggregate into an ellipse. Monte-Carlo simulations indicated that the site heterogeneity within a complex (Γ_{intra}), defined as the full width at half maximum (FWHM) of a Gaussian distribution of site energies, was approximately the same as the interaction strength (Ketelaars et al., 2001). Under these conditions the excited states are delocalized over a substantial part of the ring (Alden et al., 1997; Mostovoy and Knoester, 2000). The large bandwidths of the bands reflected the short lifetime of these states due to fast exciton relaxation. For 3 of 19 spectra of individual LH2 complexes a narrow absorption line on the low-energy side of the $k^{\mathrm{circ}} = \pm 1$ bands was observed. This low-energy state was assigned to the long-lived emitting state $k^{\mathrm{circ}} = 0$, and its observation is another indication that the circular exciton model is applicable for LH2.

It would be very attractive if similar experiments could be carried out on the LH1-reaction center (RC) complex to understand the efficient energy transfer within this complex as well as from LH1 to the RC. The idea is that the optically excited states of LH1 are also characterized by excitonic interactions and that its spectroscopic features reveal the spatial organization of the subunits in the LH1 ring. For example, the presence of an open ring structure as discussed by Cogdell et al. (1996), instead of a closed one, will have implications for the structure of the manifold of excited states. To observe the detailed spectroscopic structure of the exciton states and to relate this information to structural parameters, it is imperative to perform experiments at the single-complex level.

In this paper we describe the results of the single-molecule experiments that we performed on LH1-RC core complexes of *Rps. acidophila* at low temperature. The experimental observations are distinctly different from those of LH2. Evidence for a circular exciton is much less pronounced in the case of LH1. The observed spectra show a large variation in terms of the number of bands and their polarization behavior, indicating that besides site heterogeneity also structural heterogeneity is likely to play a role. This leads to the conclusion that the LH1 ring in the LH1-RC complexes of *Rps. acidophila* is not fully intact in many of the complexes that were examined. Further research should reveal if such heterogeneity is a native property of the complex.

Current structural models for LH1

For LH1, it has not been possible yet to obtain high-quality crystals, and therefore the three-dimensional arrangement of its subunits remains to be ascertained. This is in contrast to the structures of two LH2 complexes (McDermott et al., 1995; Koepke et al., 1996) and one LH3 complex (McLuskey et al., 2001), which have been resolved by x-ray crystallography. These structures reveal a highly symmetric, closed, circular arrangement consisting of nine (McDermott et al., 1995; McLuskey et al., 2001) or eight (Koepke et al., 1996) subunits. From these and other biochemical studies (Zuber and Cogdell, 1995), it has been established that the structure of the various antenna complexes of purple bacteria are all based on a similar modular principle, each module consisting of a pigment-protein subunit. Such a subunit contains a pair of transmembrane polypeptides (α and β), binding two (LH1) or three (LH2, LH3) BChl pigments. Of the three pigments in the LH2 and LH3 subunit, one contributes to the absorption ~800 nm and is spatially distinct from the other two pigments. The latter are tightly coupled and absorb ~820 nm in the case of LH3 and 850 nm for LH2. Based on the homology between the LH1 and LH2 proteins, the LH1 subunit is believed to contain only two coupled pigments, contributing to its absorption band ~870 nm (Visschers et al., 1991).

Pigment analysis of LH1-RC complexes showed that the number of BChl *a* molecules per LH1 varied from 23 to 33 for different strains of purple bacteria (Francke and Amesz, 1995; Gall, 1995; Qians et al., 2000). These values are higher than the number of 16 to 18 pigments that are present in the B850 ring of LH2 and the B820 ring of LH3. Together with the large homology of the protein subunits,

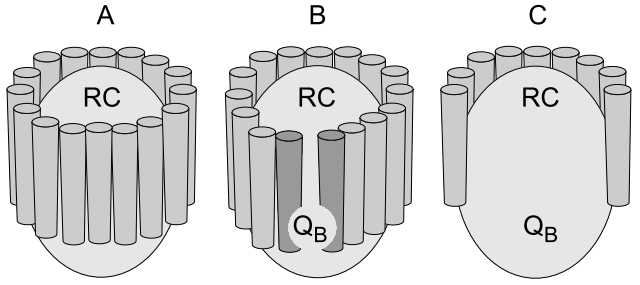

FIGURE 1 Three tentative structural models for the LH1-RC complex. The $\alpha\beta$-subunits of the LH1 are depicted as cylinders. Q_b represents the secondary quinone site of the RC. (*A*) A closed-ring model with the LH1 ring, consisting of 16 $\alpha\beta$-subunits, completely surrounding the RC and blocking the Q_b site. (*B*) A LH1 model with incorporation of the PufX protein represented as a dimer substituting 2 $\alpha\beta$ subunits. The PufX protein may facilitate ubiquinone transfer from the Q_b site. (*C*) An open-ring model, consisting of 8 $\alpha\beta$-subunits in which the Q_b site is exposed. Adapted from Cogdell et al. (1996).

this could indicate that the main difference between LH2 and LH1 is the size of the ring. This view is supported by electron-microscopy experiments on LH1 complexes of both *Rhodospirillum* (*Rsp.*) *rubrum* (Karrasch et al., 1995) and *Rhodobacter* (*Rba.*) *sphaeroides* (Walz et al., 1998). These experiments showed the two-dimensional (2-D) projection structures of reconstituted LH1 complexes, consisting of a closed-ring structure of 16 $\alpha\beta$-subunits, which is just large enough to incorporate an RC in the core of the ring (Karrasch et al., 1995; Cogdell et al., 1996). In Fig. 1 *A* a schematic representation of such an LH1-RC arrangement is depicted. Earlier electron-microscopy data of *Rba. viridis* (Stark et al., 1984) and of *Rps. marina* (Meckenstock et al., 1992) also showed a closed-ring structure for LH1.

Nevertheless, the general validity of a closed-ring model may be questioned for various reasons. First of all, the pigment analyses indicate that in many strains the number of pigments in LH1 per RC may be much lower than 32, i.e., too small to incorporate an RC in its core. Second, the 2-D crystals of *Rsp. rubrum* involved LH1 complexes, which were reconstituted from $\alpha\beta$-dimers obtained by detergent treatment of the native LH1 complex (Ghosh et al., 1993; Karrasch et al., 1995). Therefore, it is unclear to what extent they are representative of the structures in the native membrane or even of isolated LH1 or LH1-RC complexes. For the experiments on *Rba. sphaeroides* (Walz et al., 1998) a mutant was used lacking the *pufX* gene (see below). Such a mutant is incapable of photosynthetic growth (McGlynn et al., 1994), which may well affect the structure of the photosynthetic apparatus. Noncircular structures of LH1 have also been reported. For example, other electron-micrograph studies indicated an open, C-shaped dimeric structure of LH1 (Jungas et al., 1999) in membranes of *Rba. sphaeroides*, whereas in *Rsp. rubrum* the image analysis of 2-D crystals of LH1-RC complexes revealed an almost square LH1 structure (Stahlberg et al., 1998). The latter complex was found to contain an additional protein, the Ω-peptide (Ghosh et al., 1994), but it could not be resolved in the 2-D crystals.

An additional, small transmembrane protein, called PufX has also been found in the case of *Rba. sphaeroides* and *Rba. capsulatus* (Farchaus et al., 1992; Lilburn et al., 1992; Recchia et al., 1998; Parkes-Loach et al., 2001). Both PufX and the Ω-peptide are thought to form an integral part of the LH1 ring (Cogdell et al., 1996; Stahlberg et al., 1998). The PufX protein is required for photosynthetic growth (Farchaus et al., 1992; Lilburn et al., 1992; Barz et al., 1995a) and may facilitate migration of the quinone towards the cytochrome bc_1 complex by forming a specific channel or passage through the ring of LH1 (Lilburn et al., 1992; Barz et al., 1995b; McGlynn et al., 1996). However, this requirement of PufX is relaxed when the LH1 complex is either absent (McGlynn et al., 1994) or reduced in size (McGlynn et al., 1996). LH1 is approximately 2 subunits per RC larger when PufX is absent (McGlynn et al., 1994). Recent linear-dichroism measurements on oriented membranes of *Rba. sphaeroides* indicated that PufX plays a role in the orientation of the RC in the LH1 ring as well as in the formation of long-range regular arrays of LH1-RC cores (Frese et al., 2000). This result supports the presumed portal function of PufX. In Fig. 1 *B* the PufX model for the LH1-RC complex is schematically depicted, where a dimeric PufX substitutes two subunits of the LH1 ring (Cogdell et al., 1996). In species with no PufX, other proteins like the Ω-peptide in the case of *Rsp. rubrum*, might have a similar function.

There is no direct structural evidence that PufX, the Ω-peptide, or other membrane proteins form an integral part of the LH1-RC core complex. Moreover, PufX and the Ω-peptide have both not been found in *Rps. acidophila*, but it is not known if there is another protein as part of the LH1 ring in this species with a similar function. Alternatively, it is possible that in this case LH1 is not a closed but an open ring, because then the photosynthetic growth is not impaired as concluded from the experiments on *Rba. sphaeroides.* In Fig. 1 *C* such a model is depicted.

It should be realized that the models for the LH1-RC complexes shown in Fig. 1 have been proposed in the absence of a detailed insight of their structure by high-resolution x-ray study. Indications of an open-ring structure, which might or might not be closed by additional proteins, suggest that the spatial organization of LH1 is subjected to a larger variation in structure and composition than LH2, at least in vitro. We will refer to this variability as structural heterogeneity. Moreover, the results depend strongly on the species examined, the mutations introduced and the (biochemical) history of the sample. For example, LH1-RC complexes are much more unstable in detergent solution than LH2 complexes (Hawthornthwaite and Cogdell, 1991). The motivation for optical spectroscopy measurements on individual LH1 and LH1-RC complexes is that such exper-

iments can elucidate structural heterogeneity and variations by correlating the electronic structure derived from the optical spectra with the spatial arrangement of pigments in the LH1 complex.

MATERIALS AND METHODS

The LH1-RC complexes of *Rps. acidophila* (strain 10050) were prepared as described elsewhere (Law, 1998). The presence of the RC is thought to preserve the integrity of the LH1 complex. The LH1-RC complexes were diluted up to 5×10^{-11} M in buffer (10 mM Tris, 0.1% lauryldimethylamine *N*-oxide, 1 mM EDTA, pH 8.0) with 1 % (wt/wt) purified polyvinyl alcohol (Ketelaars et al., 2001) present. The primary donor of the RC was not preoxidized and therefore believed to be still photochemically active. A drop (10 μL) of the solution was spincoated on a LiF substrate by spinning it for 15 s at 500 rpm and 60 s at 2000 rpm, producing high-quality films with a thickness of less than 1 μm. The samples were mounted in a liquid-helium cryostat and cooled to 1.2 K.

To perform fluorescence microscopy and fluorescence-excitation spectroscopy the samples were illuminated with a continuous-wave tunable Ti:Sapphire laser (Spectra Physics, Mountain View, CA). A fluorescence-excitation spectrum of an individual LH1-RC complex was obtained in two steps. First a wide-field image was taken of the sample by exciting at 870 nm and detecting fluorescence at 910 nm with a CCD camera (Princeton Instruments, Trenton, NJ). From this image a spatially well-isolated complex was selected. Next, a fluorescence-excitation spectrum of this complex was obtained by switching to the confocal mode of the set-up and scanning the excitation wavelength, while detecting fluorescence at 910 nm with an avalanche photodiode (EG&G, Quebec, Canada). The detection bandwidth was 20 nm.

To assess and minimize the effect of spectral diffusion (van Oijen et al., 1999a, 2000), the spectra were obtained in rapid succession by repetitive scans of the whole spectral range and storing the different traces separately. With a scan speed of the laser of 3 nm per second and an acquisition time of 10 ms per data point, this yields a nominal resolution of 0.5 cm^{-1} ensuring that the spectral resolution is limited by the spectral bandwidth of the laser (1 cm^{-1}). For more experimental details see van Oijen et al. (1999b). To examine the polarization dependence of the spectra, a ½λ plate was put in the confocal excitation path. This plate could be rotated in steps of 1.8°. As a consequence the angle of polarization of the excitation light was changed with twice the step size. A total of 24 complexes was studied.

To simulate the optical spectra, a model for the pigment arrangement of the three-dimensional structure of the LH1 complex was used by assuming a closed-ring structure consisting of 16 $\alpha\beta$-subunits (Karrasch et al., 1995). The distances between the pigments in the LH1 ring and their mutual orientations were taken to be identical as in LH2 (McDermott et al., 1995). The atomic co-ordinates of LH2 of *Rps. acidophila* were taken from the Brookhaven Protein Data Bank (1kzu.pdb). The electronic structure of the LH1 ring was approximated using only the lowest (Q_y) excited states of the individual BChl *a* molecules. The interactions between the pigments were calculated using a simple point-dipole approximation (Pearlstein, 1991; Sauer et al., 1996). This resulted in nearest-neighbor interactions of 253 and 229 cm^{-1} for the intra- and interdimer interaction, respectively. All interactions up to second neighbor were included. The site-energy of the β-bound pigments was taken to be 11,800 cm^{-1}. Due to a slightly different environment of the α- and β-bound pigments, the transition energies of the α-bound pigments were taken to be 240 cm^{-1} higher (see also Ketelaars et al., 2001).

RESULTS

In Fig. 2 *a* the fluorescence-excitation spectrum of an ensemble of LH1-RC complexes in a PVA film is depicted

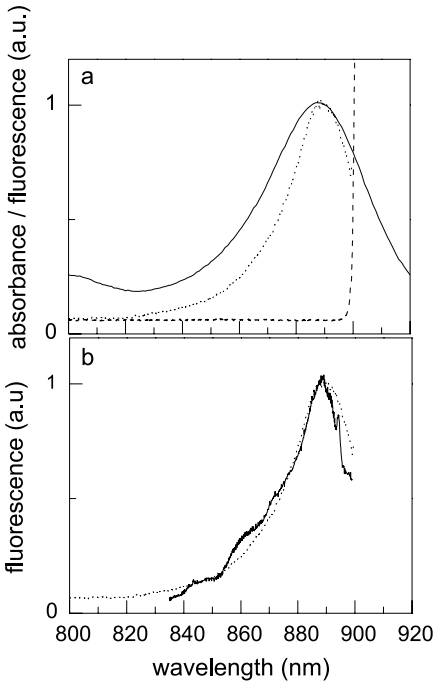

FIGURE 2 Ensemble spectra of LH1-RC complex of *Rps. acidophila.* (*a*) Room-temperature absorption spectrum in solution (*solid line*) and the fluorescence-excitation spectrum at 1.2 K of a high-concentrated sample with 1% PVA spincoated onto a LiF substrate (*dotted line*). The dashed line indicates the transmission of the filter used in the emission path (center, 910 nm; FWHM 20 nm). (*b*) Fluorescence-excitation spectrum of a bulk ensemble of LH1-RC complexes in a PVA-film at 1.2 K (*dotted line,* same as in *a*) together with the sum of 24 spectra recorded from individual complexes (*solid line*). The spectrum of each individual complex was obtained at 1.2 K in a PVA film at an intensity of 2 to 10 W/cm^2. The spectra are scaled to the same intensity.

(dotted line). The fluorescence-detection window is centered at 910 nm with a FWHM of 20 nm and coincides with the emission band of the ensemble spectrum under PVA-film conditions. The spectrum was obtained at 1.2 K and shows a narrowing of the Q_y band compared with that at room temperature as was also reported for LH2 and LH1 (Wu et al., 1997, 1998). The maximum of the band is shifted by ~3.5 nm to the red compared with the room-temperature spectrum (solid line). Fig. 2 *b* shows a comparison of the ensemble spectrum (dotted line) and the sum spectrum of 24 individual complexes (solid line). The sum spectrum is slightly blue shifted compared with the ensemble spectrum and also the blue wing of the band shows a small difference.

In Fig. 3 the fluorescence-excitation spectra of eight different individual LH1-RC complexes out of a total of 24 observed individual complexes are depicted. The experimental protocol was basically the same as reported previously (Ketelaars et al., 2001). The spectra are averages over all possible excitation polarizations. They show large differences when comparing the number of bands, bandwidths, and intensities. However, in all spectra broad absorption bands are observed with widths ranging from 150 to 200

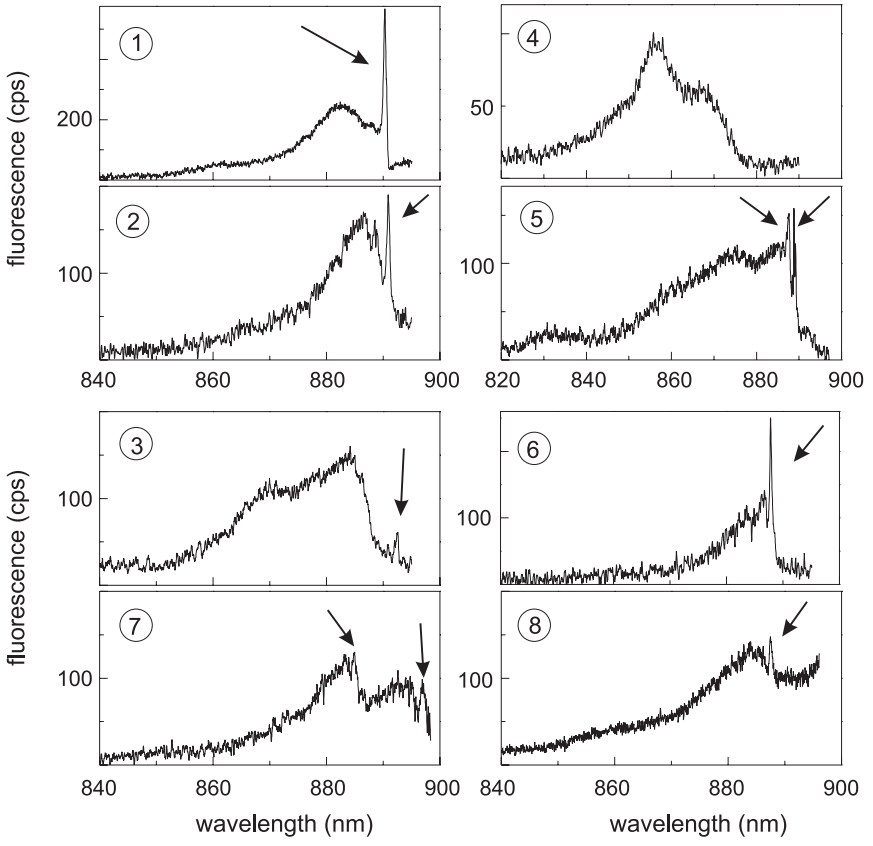

FIGURE 3 Eight examples of fluorescence-excitation spectra of individual LH1-RC complexes of *Rps. acidophila.* Each individual complex was studied at 1.2 K in a PVA-film at an intensity of 2 to 10 W/cm^2. The arrows point towards the narrow absorption lines present in some of the spectra.

cm^{-1} indicating dephasing times of tens of femtoseconds. Almost all spectra have their main absorption bands around 880 to 890 nm. Most spectra show absorption intensity over a range of roughly 40 nm (~500 cm^{-1}). Although the substructure is evident, in some spectra the broad bands are not well resolved, and therefore it is difficult to determine the exact number of bands in these cases.

Most spectra (80%) show also narrow absorption lines (complexes 1–3, 5–8). The intensities of these lines vary from complex to complex. For most of these lines the signal-to-noise ratio is good enough to determine their width within one scan, reducing the influence of spectral diffusion. The widths of these narrow features are approximately 1 to 3 cm^{-1} and are mainly determined by the spectral width of the laser excitation source (1 cm^{-1}). The spectral positions of the narrow lines are always on the red wing of a broad absorption band. Some spectra show two narrow lines as can be seen in the spectra of the complexes 5 and 7. In such cases another broad absorption band may be present on the red side of a narrow line (complex 7). Occasionally a part of the spectrum overlaps with the detection window (complex 8), possibly masking a second narrow line at the long-wavelength edge.

To determine the mutual orientation of the polarization of the bands, the angle of the linearly polarized light was rotated by 3.6° after each scan, using a ½λ plate. The additional advantage is that bands and shoulders in the optical spectra could be resolved more easily, allowing a more accurate determination of their shape and position. As an example, we show in Fig. 4 the effect of the rotation of the excitation polarization on the spectrum of complex 1 of Fig. 3. For this particular complex four different bands can be distinguished, labeled 1 to 4 as seen in Fig. 4 *a* (bottom) and identified each by its own polarization dependence of the absorption. The emission intensity is indicated by the grey scale (white: high intensity). After the polarization is rotated 180° (*y* axis), the typical absorption pattern that is observed for these four bands repeats itself. In total 300 scans or five complete turns of the excitation polarization were typically recorded.

The bottom part of Fig. 4 *a* shows the average over all scans. For each observed band (1–4) of this particular complex, a small spectral region was selected around its center wavelength and the total intensity of this region was plotted against the excitation polarization (Fig. 4 *b*; top). The intensity traces for each band were fitted with a cos^2 dependence (not shown) giving the polarization of the band at maximum intensity and its phase. The phase differences of the bands give the relative orientation of the transition moment, which in this case corresponds to 88 ± 3°. The optical spectra associated with the nearly orthogonally polarized bands are plotted in the lower panel of Fig. 4 *b.* In

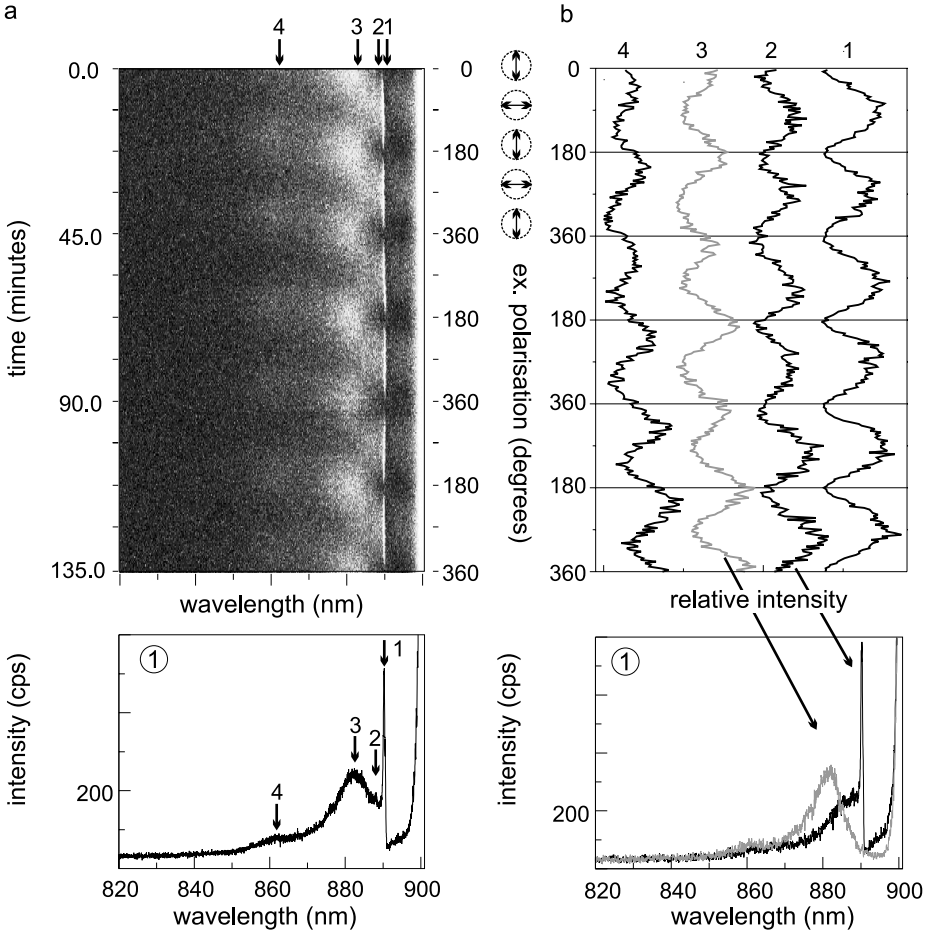

FIGURE 4 Fluorescence-excitation experiment on an individual LH1-RC complex (number 1) of *Rps. acidophila* at 1.2 K. (*a, Top*) Stack of 300 fluorescence-excitation scans recorded at a scan speed of 3 nm/s. After each scan, corresponding to one horizontal line, the excitation polarization was rotated by 3.6° (see Materials and Methods). The series of scans correspond to five complete turns of the polarization. The fluorescence intensity is indicated by the grey scale (white; high intensity). (*a, Bottom*) Average of the 300 individual scans. The numbers 1 to 4 indicate the four different bands that were observed for this particular complex. (*b, Top*) The relative intensity of the four bands as a function of the excitation polarization. From the phase difference between these oscillations the mutual polarization of the bands was determined. (*b, Bottom*) The two spectra of band 2 and 3 plotted at their maximum intensity. Their mutual orientation was 88 ± 3°. No data processing was done except for averaging of three adjacent points. The encircled bidirectional arrows in the center of the figure indicate the polarization of the excitation light. No background was subtracted, and therefore the transmission of the detection window is visible in the red edge of the spectrum.

the sequence of polarized spectra, bands 2 and 3 can clearly be resolved despite their strong overlap.

Based on the polarization behavior and additional spectral features, the different LH1-RC complexes can be roughly divided into four different types labeled I to IV. An example of each type is depicted in Fig. 5. In Table 1 the spectroscopic details of the type I spectra are summarized. The spectra belonging to type I are dominated by two broad bands around 870 to 880 nm. The polarization of these bands is mutually orthogonal within 6° (Table 1). Such a polarization pattern is very similar to that observed for the LH2 complex (van Oijen et al., 1999a; Ketelaars et al., 2001) and we will tentatively assign the two bands to the lowest degenerate states of a circular exciton denoted by their quantum number $k^{\mathrm{circ}} = \pm 1$. The degeneracy of these two states is lifted. Occasionally the spectra show a narrow absorption line on the low-energy site of the $k^{\mathrm{circ}} = \pm 1$ states (Fig. 3), which we think represents the long-lived emitting state, $k^{\mathrm{circ}} = 0$. Like in the LH2 spectra, the larger separations between the $k^{\mathrm{circ}} = \pm 1$ states ($\delta E_{\pm 1}$) are dominant. The average values of $\delta E_{\pm 1}$ for the LH1-RC and LH2 (Ketelaars et al., 2001) complexes are roughly the same, respectively 116 ± 77 cm^{-1} and 110 ± 39 cm^{-1} (Table 1). The average energy separation $\delta E_{1|\mathrm{k}|}$ of 418 ± 129 cm^{-1} between the spectral mean of the $k^{\mathrm{circ}} = \pm 1$ states and the band at higher energy is much larger for the LH1-RC than reported for the LH2 spectra (285 ± 35 cm^{-1}) (Ketelaars et al., 2001). The $k^{\mathrm{circ}} = 0$ state is much more pronounced than in the LH2 case and is detected more often, i.e., in five of the seven type I spectra. Of the 24 observed individual LH1-RC spectra only 30% of the spectra exhibit a type I pattern. This is in contrast to the individual LH2 spectra, where all of the 19 complexes studied showed two orthogonal bands, indicative for a circular exciton.

The spectra of type II show two broad bands with a mutual angle of polarization significantly less than 90° (Fig. 5; type II). The angles vary between 30 to 64°. Two spectra show a narrow absorption line on the low-energy side of the spectrum. Table 2 summarizes the spectral details. Despite the fact that the mutual orthogonality of the two broad bands is not maintained, we believe that these states might still represent the lowest degenerate states of a circular exciton. We, therefore, label them "k^{circ}". Seventeen percent of the complexes (four in total) exhibit this behavior. If the angle is significantly less than 90°, it is more difficult to determine the mutual polarization of the two bands and their spectral position is not so well resolved at any polarization. Therefore, the values in Table 2 are less accurately determined.

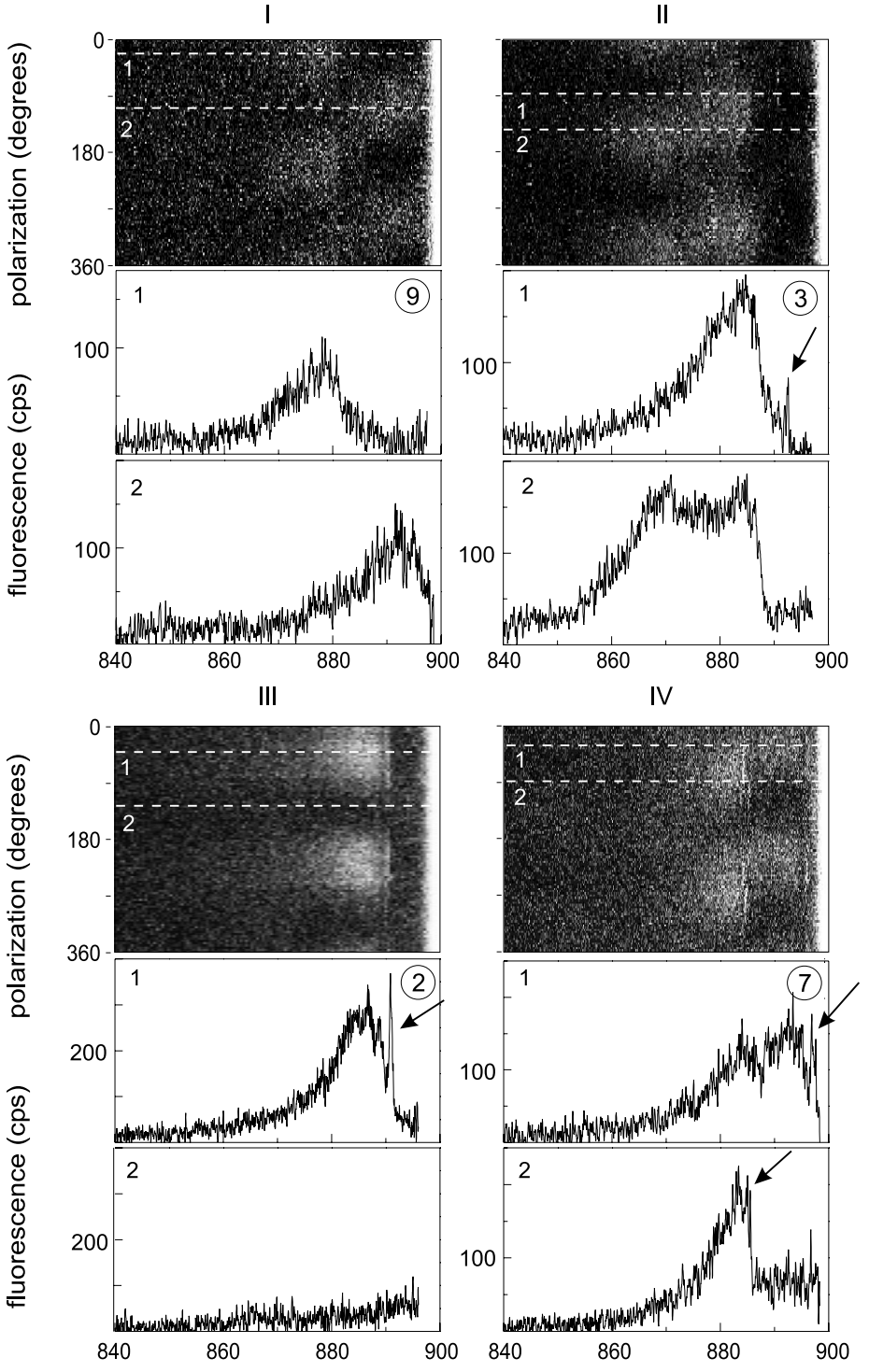

FIGURE 5 Four different types of polarization behavior of the fluorescence-excitation spectra of individual LH1-RC complexes (*Rps. acidophila*). The upper panels in **I, II, III,** and **IV** show a stack of 100 fluorescence-excitation scans. After each scan the excitation polarization was rotated by 3.6° (see Materials and Methods). The fluorescence intensity is indicated by the grey scale (white; high intensity). Five complete turns of the polarization were made in successive scans, although only two turns are shown. The two spectra at the bottom of **I, II, III** and **IV** are taken at a specific polarization, indicated by the two white dashed lines in the corresponding upper panel. Experimental conditions as in Fig. 3. The encircled numbers indicate the particular complex chosen. In **I** two broad orthogonal bands are observed that show the same behavior as for complex 1 (Fig. 4). In **II** two broad bands are present with a mutual angle of less than 90°. In **III** one broad band is observed with no absorption at the perpendicular polarization. In **IV** multiple narrow lines are observed. The arrows point towards the narrow absorption lines present in some of the spectra.

A third type (III) of complexes shows a behavior as depicted in Fig. 5; type III. Their characteristic property is that there are angles of polarization without any detectable absorption. By comparing the optical spectra taken at polarizations of 45° (spectrum 1) and 135° (spectrum 2), respectively, this becomes even more obvious. It should be pointed out that the narrow line in the red edge of the spectra has the same polarization as the broad band. In Table 3 the spectroscopic details are summarized. Seventeen percent of the total number of complexes belong to this group.

The last type (IV) shows two narrow absorption lines that are each located on the red edge of a broad absorption band (Fig. 5; type IV). They are visible in the two spectra 1 and 2, which have been taken at different polarizations. The

TABLE 1 Spectroscopic details of the individual LH1-RC spectra belonging to type I (Fig. 5)

No.	$k^{circ} = \pm 1$ S.P. (nm)		$\delta E_{\pm 1}$ cm^{-1}	$\phi_{\pm 1}$(degrees)	$\lvert k^{circ}\rvert > 1$ S.P. (nm)	$k^{circ} = 0$ S.P. (nm)	$\delta E_{1\lvert k\rvert}$ (cm^{-1})	δE_{01} (cm^{-1})
LH1-RC (*Rps. acidophila*)								
1	882	888	76	88	862	890.3	301	67
9	877	893	204	85	858*	–	355	–
10	878	890	153	88	–	894.0	–	126
11	889	891	25	83	858*	893.5	419	44
12	885	893	101	82	–	897.0	–	100
13	884	887	38	87	–	892.1	–	84
14	876	893	217	83	840	–	598	–
Mean ± SD	882 ± 4.7	891 ± 2.5	116 ± 77	85 ± 2.5	855 ± 9.8	893 ± 2.5	418 ± 129	84 ± 31
LH2 (*Rps. acidophila*) (Ketelaars et al., 2001)								
Mean ± SD	856 ± 5.7	864 ± 4.8	110 ± 39	90†	841 ± 3.3	862 ± 2.3	285 ± 35	84 ± 23

*Weak band; †within the accuracy of the experiment the angle was always 90°.

The two, mutual orthogonal, broad bands are tentatively assigned to $k^{circ} = \pm 1$ states of a circular exciton and the narrow absorption line in the most red part of the spectrum to the $k^{circ} = 0$ state. For comparison the averaged spectroscopic details of the individual LH2 complexes are summarized at the bottom. S.P. stands for the spectral position of the bands and SD for the standard deviation. $\delta E_{\pm 1}$ indicates the energy separation between the $k^{circ} = \pm 1$ states. $\phi_{\pm 1}$ the angle between the directions of the polarization of these states. $\delta E_{1|k|}$ indicates the energy separation between the spectral mean of the $k^{circ} = \pm 1$ states and the higher exciton state indicated by $|k^{circ}| > 1$. δE_{01} is the energy separation between the spectral mean of the $k^{circ} = \pm 1$ states and the $k^{circ} = 0$ state.

relative angle of polarization of the two broad bands for this particular complex is approximately 50°. Other complexes in this group show angles that are significantly different. Complexes with a narrow line in the middle of the their spectrum and a broad band on the red side extending in the detection window also belong to this group, since the detection window could be masking a second narrow line (e.g., complex 8). In total 36% of the studied complexes exhibit a type IV behavior.

DISCUSSION

It is very gratifying that it proves possible to observe the fluorescence-excitation spectra of the individual LH1-RC complexes. The experiments rely on the fact that quenching of fluorescence by the RC, which is known to be very efficient for both open and closed centers (Freiberg, 1995 and references there in) does not play a significant role in our case. This is in line with earlier temperature-dependent fluorescence measurements on whole cells of *Rps. rubrum*, which indicated that at 4 K the fluorescence yield for both open and closed RCs is much higher than at room temperature (Rijgersberg et al., 1980). An explanation for this effect was given in terms of the site heterogeneity of the LH1 complex. Especially at low temperature the lowest energy level of a significant fraction of the LH1 complexes is thought to be shifted to the red with respect to the energy level of the primary donor (P) of the RC, thus enhancing fluorescence from LH1 because of reduced trapping efficiency (Valkunas et al., 1992; Somsen et al., 1994).

The two most pronounced features of the fluorescence-excitation spectra of the individual LH1-RC complexes of *Rps. acidophila* is the observation of a limited number of bands with a characteristic polarization behavior and a large variation in their appearance. In general three to four bands (broad and narrow) are observed in one spectrum. Even when counting the shoulders in some cases as separate bands, no spectrum shows more than six bands. This small number suggests that the "ring of dimers" model (van Mourik et al., 1992; Visser et al., 1995; Bradforth et al., 1995; Jimenez et al., 1997) is less appropriate to describe the optical properties of individual LH1-RC complexes, at

TABLE 2 Spectroscopic details of the individual LH1-RC spectra (*Rps. acidophila*) belonging to type II (Fig. 5)

No.	"$k^{circ} = \pm 1$" S.P. (nm)		$\delta E_{\pm 1}$ (cm^{-1})	$\phi_{\pm 1}$ (degrees)	"$\lvert k^{circ}\rvert > 1$" S.P. (nm)	"$k^{circ} = 0$" S.P. (nm)	$\delta E_{1\lvert k\rvert}$ (cm^{-1})	δE_{01} (cm^{-1})
3	870	883	170	42	842	890.3	467	177
4	857	868	148	30	–	–		
15	881	887	77	45	–	894.0		127
16	876	886	129	64	855*	–	345	–
Mean ± SD	871 ± 10	881 ± 8.8	131 ± 40	45 ± 14	847 ± 7.1	893 ± 1.4	406 ± 86	152 ± 35

*Weak band.

The different parameters are described in the caption of Table 1.

TABLE 3 Spectroscopic details of the individual LH1-RC spectra (*Rps. acidophila*) belonging to type III (Fig. 5), which is dominated by a broad band around 880 nm and a narrow line at lower energy

	Broad band	Narrow line
No.	S.P. (nm)	S.P. (nm)
2	885	890.8
6	887	888.5
18	877	–
19	871*	–
Mean ± SD	880 ± 7.4	889.7 ± 1.6

*Accompanied by a weak band at 840 nm.
The mutual polarization of the two bands is the same. S.P. stands for the spectral position of the bands and SD for the standard deviation.

least at low temperature. In such a model the total number of bands would be much larger, assuming a LH1 structure with 16 subunits. Also the fact that most spectra do show one or two preferred polarization directions does not support the "dimer model." Therefore, we believe that the spectroscopic features are better described in terms of a collective excitation of the complete ring. Hence, we will discuss the optical properties of the LH1 complex in terms of circular Frenkel excitons, i.e., we assume that the set of excitonic eigenstates of the full ring determines the spectra of the individual LH1 complexes.

The variation in the fluorescence-excitation spectra manifests itself in the number of bands, their polarization behavior, bandwidths, and spectral positions (Fig. 3–5). A large part of the complexes (80%) shows a narrow absorption line. In addition, 20% of the spectra show multiple narrow absorption lines (Fig. 3). All spectra show broad bands, indicating dephasing times of tens of femtoseconds with a clear dependence on the polarization of the excitation light (Fig. 5). Because most of the observed bands are broad (150–200 cm^{-1}), it is not always possible to resolve all the bands in the spectrum. Based on the polarization behavior and number of bands we can distinguish four groups of spectra, labeled I to IV (Fig. 5). The first group (I) shows two broad bands with a mutual orthogonal polarization. The second group (II) also shows two broad bands but with a mutual orientation, which deviates significantly from 90°. The third group (III) is characterized by a single, linear polarization of the whole spectrum. The fourth group (IV) shows two narrow features in one spectrum.

To understand these observations, it should be realized that the excitation spectra of the individual complexes are strongly influenced by site heterogeneity, structural heterogeneity, and the orientation of the complexes in the polymer film. These three effects are mutually not exclusive and it is likely that the properties of each group of spectra is determined by a combination of all three. The presence of the RC is not expected to influence the electronic structure of LH1 significantly, because the distance between the primary donor (P) and the pigments of the LH1 ring of ~ 43 Å (Papiz et al., 1996) reduces the coupling between P and LH1 (Novoderezhkin and Razjivin, 1994). The mismatch between the energy of P and the lowest state of LH1 will further reduce the effect of this coupling. The RC does act as a mould for the LH1 ring (compare with Fig. 1) and may therefore induce structural distortions in the circular symmetry of this ring. Because the RC has a twofold symmetry, it could induce a twofold structural deformation of LH1. Such a deformation will have great implications for the electronic structure (Matsushita et al., 2001; Ketelaars et al., 2001).

To gain further insight in the implications of both site and structural heterogeneity on the optical spectrum of an individual LH1 complex, we performed a series of numerical simulations. A ring size of 16 subunits was assumed with identical interactions within and between these units as in the B850 band of LH2. Frenkel-exciton theory for such a closed-circular arrangement predicts that for a perfect symmetry all oscillator strength in the plane of the ring is concentrated in the lowest pair of degenerate exciton states, denoted by their quantum numbers $k^{\mathrm{circ}} = \pm 1$. Because of the circular symmetry, the transitions to these states can be decomposed into two linearly polarized components of equal oscillator strength. The direction of their transition-dipole moments can be in any direction within the plane of the ring, but they are always mutually orthogonal (see, e.g., Matsushita et al., 2001).

The introduction of site heterogeneity will, first of all, cause mixing of the different exciton levels and a redistribution of oscillator strength to nearby states, including the lowest, nondegenerate $k^{\mathrm{circ}} = 0$ state (Ketelaars et al., 2001). Because this lowest energetic state has a relatively long lifetime it appears in the most red part of the optical spectrum as a narrow absorption line. Second, it modifies the spacing between the exciton levels and removes the pair-wise degeneracy. The mutual orthogonality of the $k^{\mathrm{circ}} = \pm 1$ states is fairly conserved, although for an ensemble of complexes it shows a distribution of angles centered around 90° (Alden et al., 1997; Ketelaars et al., 2001). The width of such a distribution depends on the extent of site heterogeneity.

The redistribution of oscillator strength among adjacent exciton levels depends on both the relative extent of site heterogeneity as well as the energy separation of the exciton levels. In LH1 the density of states is almost twice as high as in LH2, because it scales approximately with the number of pigments for the same width ($\sim 4\ V_{\mathrm{avg}}$) of the exciton manifold. This implies a smaller energy separation between adjacent exciton states and therefore a stronger mixing of these states as a result of disorder. This effect is depicted in Fig. 6 for a circular array of strongly-interacting pigments of two different sizes, i.e., 18 (Fig. 6 *a*) and 32 (Fig. 6 *b*), which represent LH2 and LH1, respectively. The left part of Fig. 6 *a* and *b* shows the lower part of the exciton manifold without site heterogeneity. In this case the optical spectra of

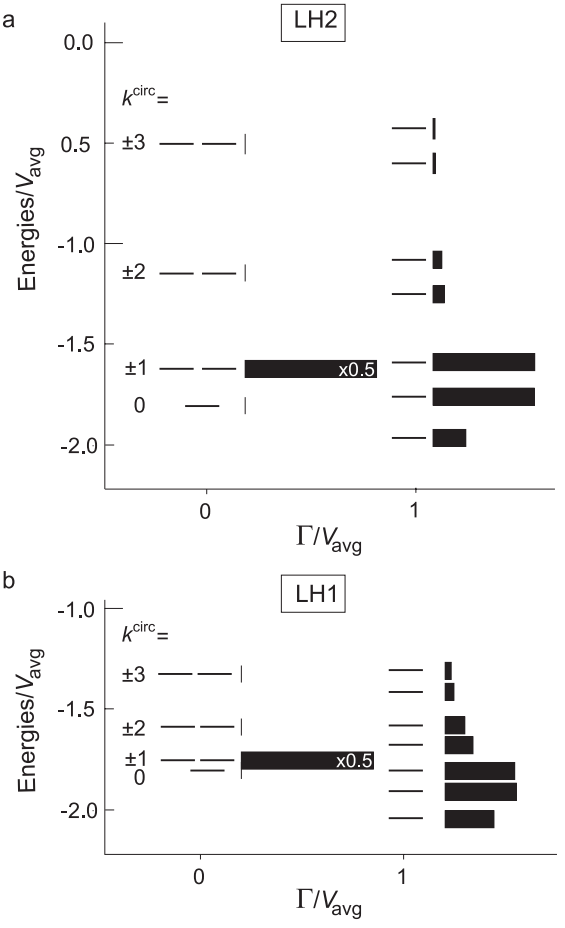

FIGURE 6 Simulation of the excited state energies of both LH2 (*a*) and LH1 (*b*). Only the lowest part of the exciton manifold is depicted. For LH2 the atomic co-ordinates of *Rps. acidophila* were used consisting of 18 pigments with a C_9 symmetry (1kzu.pdb). For LH1 a closed-ring model was used consisting of 32 pigments with a C_{16} symmetry. The mutual distances and orientations of the pigments were taken to be the same as in LH2 (*Rps. acidophila*), resulting in the same intra en interdimer interaction strengths. The left part of both figures depicts the manifolds without site heterogeneity. The right part is obtained with the introduction of site heterogeneity with $\Gamma_{intra}/V_{avg} = 1$. Γ_{intra} is defined as the full width at FWHM of a Gaussian distribution of site energies within a complex. V_{avg} is the average of the inter- and intradimer interaction between the pigments. The transition probabilities from the ground state to the various excited states of the exciton manifold are depicted by the length of the black bars. In the presence of site heterogeneity averaging over 10,000 complexes was performed. See Material and Methods for a more detailed description of the simulations. Note that the LH2 manifold is only shown for comparison to the LH1 case and does not match the exciton manifold as proposed by Ketelaars et al. (2001) based on the spectra of individual LH2 complexes.

both aggregates will be the same, i.e., almost all oscillator strength will be concentrated in the two lowest degenerate states. The right part of Fig. 6, *a* and *b* shows the exciton manifolds for both aggregates after the introduction of site heterogeneity with $\Gamma_{intra}/V_{avg} = 1$. These manifolds are an average over 10,000 complexes. For the same relative extent of site heterogeneity, the distribution of oscillator strength among the *k*-states differs significantly.

Because the LH2 and LH1 complexes have such a high degree of homology in their protein subunits it is likely that the extent of site heterogeneity in LH1 is similar to that in LH2. This is in line with hole-burning experiments (Wu et al., 1998) in which the energy distribution of the lowest nondegenerate state ($k^{circ} = 0$) of the exciton manifold of LH2 and LH1 was found to have the same width within 20%. Although the site heterogeneity is assumed to be about the same, differences in the optical spectra between LH1 and LH2 are expected due to differences in the density of states. First the LH1 spectra will have stronger $k^{circ} = 0$ transitions, which as a consequence will have a higher probability to appear in the spectrum. Second owing to enhanced mixing more bands will show up in the spectrum, which are expected to overlap more strongly in the case of LH1.

To investigate the implications of the different structural arrangements proposed for LH1 (Fig. 1) on the optical properties of individual LH1 complexes, we calculated the optical spectrum of an individual LH1 complex as a function of its oligomeric structure in the absence of site heterogeneity. In Fig. 7, the results of these calculations are depicted for three different oligomeric structures corresponding to the three models A to C as proposed in Fig. 1. In Table 4 the corresponding energies and oscillator strengths of the different exciton states for these models are depicted. Model A is a complete ring of 16 subunits (Fig. 7 *A*). Model B is a ring-like structure missing one subunit, simulating the incorporation of an additional protein in the ring (Fig. 7 *B*). Model C is a half-ring structure (eight subunits) (Fig. 7 *C*). The optical transitions in the plane of the ring are depicted for both the *x* and *y* polarization with the *x* polarization corresponding to the one but lowest energetic state.

The optical spectrum of the unperturbed, complete ring of 16 subunits (Fig. 7 *A*) is dominated by the lowest degenerate states, i.e., $k^{circ} = \pm 1$. Approximately 97% of the oscillator strength is concentrated in these two, orthogonally polarized, transitions (Table 4). Because no site heterogeneity was introduced, the degeneracy of these states is maintained. The lowest state, $k^{circ} = 0$ is optically forbidden in the plane of the ring and does therefore not appear in the spectrum.

The breaking of the circular symmetry by removing an $\alpha\beta$-subunit (Fig. 7 *B*) lifts the pairwise degeneracy of exciton states. The lowest state is no longer labeled $k^{circ} = 0$, but $k = 1$ similar to that of a linear aggregate. The second state becomes $k = 2$, etc. This lowest state ($k = 1$) is no longer optically forbidden and strongly gains oscillator strength (10%), whereas its energy is slightly blue shifted (Table 4). See also the narrow feature in the red part of the spectrum (Fig. 7 *B*). The second ($k = 2$) state is virtually unchanged in both energy and oscillator strength compared with the lowest degenerate states of the ring structure (Table 4). Note that due to the smaller number of pigments its

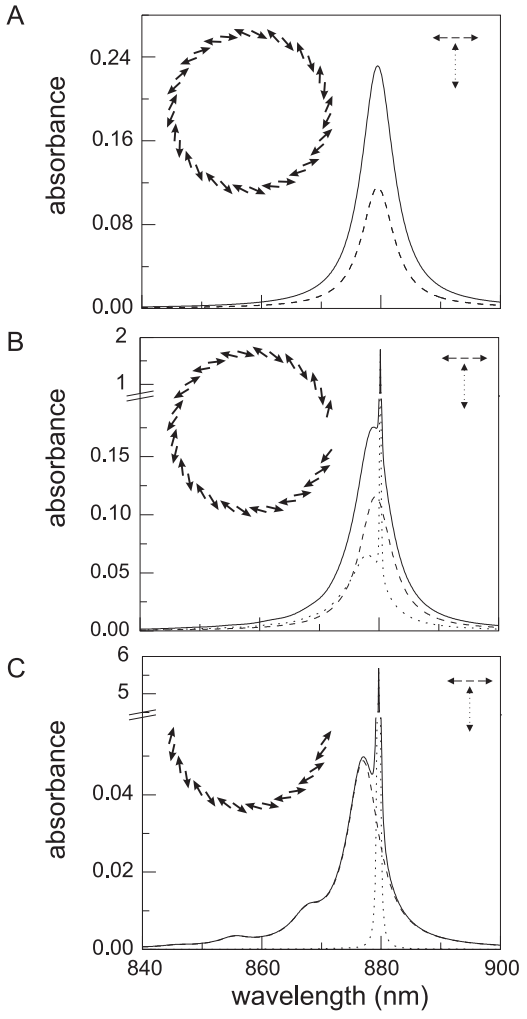

FIGURE 7 Simulation of the absorption spectrum of an individual LH1 complex, which forms a complete ring (*A*), a LH1 ring with 1 subunit missing (*B*), and a LH1 complex with a partial ring consisting of eight $\alpha\beta$ subunits (*C*). The overall absorption spectrum in the *xy* plane of the complex is plotted (*solid line*) together with the absorption spectra along the *x* axis (*dashed line*) and *y* axis (*dotted line*). The *x* axis is chosen along the transition-dipole moment of one of the $k^{\text{circ}} = \pm 1$ states in the case of A and along the $k = 2$ state in the cases B and C. The insets sketch the arrangement of the subunits in the *xy* plane, showing the Q_y transition-dipole moments (*arrows*). The lowest energetic state of the exciton manifold is assigned a homogenous linewidth of 1 cm^{-1}. All the other states 100 cm^{-1}. See Material and Methods for a more detailed description of the simulations.

relative contribution to the spectrum increases. Finally, the third ($k = 3$) state loses oscillator strength due to the curvilinear shape of the array of subunits. The energy of this state is blue shifted (1.4 nm) compared with the degenerate states of the circular arrangement (Table 4). As a consequence, the overall spectrum of such an individual LH1 is slightly blue shifted. Such a blue shift with decreasing size of the oligomeric structure was previously reported (Westerhuis et al., 1999).

When reducing the ring structure even further into a half-ring consisting of eight subunits (Fig. 7 *C*) the $k = 1$ state gains even more oscillator strength (Table 4). The $k = 2$ state still has oscillator strength, however, less than in the case with one subunit missing and is blue shifted. Due to the half-circular shape of the array, the third $k = 3$ state has almost no oscillator strength left. The two states with almost all the oscillator strength ($k = 1$ and $k = 2$) are mutual orthogonal.

In summary, the removal of subunits from the closed circular arrangement has important implications for the optical spectrum of an individual LH1 complex. Especially the increase in the oscillator strength of the lowest energetic state is remarkable. Degenerate states in the manifold are no longer present. However, the spectrum of an open ring consisting of 15 subunits will still be dominated by two, broad orthogonal bands. For a half circular arrangement also two orthogonal bands will dominate the spectrum. Because one of them represents the lowest energetic state it is likely to appear as a narrow line in the spectrum.

A problem in the analysis of the polarization dependence of the various transitions observed for the individual LH1-RC complexes in relation to the orientation of the transition dipoles in the molecular structure is the unknown orientation of the complex with respect to the exciting laser beam. In the case of individual LH2 complexes, an always perpendicular orientation of the polarization of the two $k^{\text{circ}} = \pm 1$ states was found. Apparently these complexes orient on the substrate with the plane of the ring parallel to the plane of the spin-coated sample, i.e., perpendicular to the propagation vector of the excitation beam (Ketelaars et al., 2001). A possible explanation for this orientation is the electrostatic interaction between the complex and the substrate in combination with the laminar flow induced by the spin-coating procedure. In the case of the LH1 complex the presence of the RC makes it unlikely that a similar alignment will occur. In the spatial model of the LH1-RC complex proposed by Cogdell et al. (Papiz et al., 1996; Cogdell et al., 1996) it is shown that by aligning the hydrophobic transmembrane segments of the LH1 ring (Karrasch et al., 1995) and the RC structure (Yeates et al., 1988) the RC sticks out $\sim$ 20 Å on the N terminus site of the LH1 ring. This additional protein part might tilt the plane of the LH1 ring in the polymer film. As a result the orthogonality of the $k^{\text{circ}} = \pm 1$ transitions is lost, because only a projection of these states on the plane perpendicular to the excitation beam is observed. A tilt of the ring relative to this plane will lead to a smaller mutual polarization angle of the $k^{\text{circ}} = \pm 1$ states in the recorded spectra. In the limiting case that the plane of the LH1 ring is oriented parallel to the propagation vector of the excitation light, the mutual angle of the $k^{\text{circ}} = \pm 1$ states as detected in the experiment is zero. This would imply that the LH1-RC ring structure is oriented sideways, i.e., with the plane of the ring (12-nm diameter), perpendicular to the substrate, whereas the short side of the structure

TABLE 4 Details of the simulations of the three different curvilinear models (a-c) for the LH1 ring as described in Fig. 7

Model A (16 subunits)			Model B (15 subunits)			Model C (8 subunits)		
State	Energy (nm)	o.s. (%)	State	Energy (nm)	o.s. (%)	State	Energy (nm)	o.s. (%)
$k^{circ} = 0$	880.5	0.0	$k = 1$	880.2	10.2	$k = 1$	879.6	48.1
$k^{circ} = \pm 1$	879.5	48.3	$k = 2$	879.4	51.3	$k = 2$	877.0	40.1
	879.5	48.3	$k = 3$	878.1	27.1	$k = 3$	872.9	0.2
			$k = 4$	876.2	0.1	$k = 4$	867.6	5.3
			$k = 5$	874.0	4.2	$k = 5$	861.6	0.1
			$k = 6$	871.3	0.0	$k = 6$	855.4	0.4
			$k = 7$	868.4	1.6	$k = 7$	849.7	0.3

The oscillator strength (o.s.) is taken in the plane of the ring, as a fraction of the total oscillator strength of the pigment pool. Simulation parameters are the same as in Fig. 7.

(~5.5 nm) is parallel to the substrate. Such an orientation seems highly unlikely. If the LH1-RC complexes are no longer complete rings (model C, Fig. 1), the overall protein structure could become asymmetric. The orientation of such a structure is expected to be completely different and may vary strongly between complexes. Thus, we conclude that the variation of the polarization of the transitions may very well be caused by a variation in the alignment of the complexes.

Of the four different types of spectral behavior of the LH1-RC complex, type I (Fig. 5) resembles the behavior of a circular exciton. The two broad orthogonally polarized bands around 870 to 880 nm (Table 1) are considered as a signature for circular excitonic behavior. The two bands represent the $k^{circ} = \pm 1$ states with their degeneracy lifted. The fact that the angle between the direction of polarization of these bands ($\phi_{\pm 1}$) is close to 90°, indicates that the complexes of type I are oriented with their plane parallel to the plane of the substrate. The narrow absorption line on the low-energy side of the $k^{circ} = \pm 1$ states is believed to represent the long-lived emitting state $k^{circ} = 0$ in analogy to LH2 (Ketelaars et al., 2001). This narrow line is present more often than in the case of LH2, which is most likely caused by the stronger mixing of the $k^{circ} = 0$ state with the higher $k^{circ} = \pm 1$ states because of the reduced energy separation (Fig. 6).

It would be attractive if an estimate could be made of the size of the site heterogeneity and interaction strength. Moreover, it would be interesting to investigate whether a symmetric distortion is present similar to the case of LH2 (Ketelaars et al., 2001). However, since only seven of the studied complexes belong to the type I spectra it is not possible to draw definite conclusions on both questions. We have determined the distribution of the parameter $\delta E_{\pm 1}$ (the separation of the $k^{circ} = \pm 1$ states), and $\phi_{\pm 1}$ of the spectra belonging to type I (Table 1). For these seven LH1-RC spectra the mean value of $\delta E_{\pm 1}$ is approximately the same as for LH2 and the distribution of $\phi_{\pm 1}$ is very narrow (Table 1). This suggest that these complexes are subjected to a twofold symmetric distortion of their electronic structure (Ketelaars et al., 2001; Matsushita et al., 2001). The origin of such a perturbation could be either random site heterogeneity with a strong C_2 component (Wu and Small, 1997) or a C_2 modulation of the interaction energies induced by a twofold symmetric, structural deformation of the LH1 complex (Matsushita et al., 2001). The latter model is not unlikely in view of the twofold symmetric RC, which may act as a mould for the LH1. Because the average value for $\delta E_{\pm 1}$ is about the same for LH2 and LH1, this would mean that the relative distortions of LH1 is about the same as LH2, assuming that both complexes have identical interaction strengths.

The type II spectra reveal an angle of 30 to 64° between the polarization of the two major bands. A possible explanation is that we are dealing with LH1 complexes, similar to those exhibiting type I spectra but now with the plane of the ring not oriented perpendicular to the propagation of the exciting laser beam. This different orientation might well be induced by the presence of the RC. For instance these complexes could be tilted with the protruding side of the RC oriented towards the substrate.

The type III complexes show a polarization behavior that is difficult to interpret in terms of a closed circular structure. Only an extreme, sideways orientation of the ring structure could account for the lack of absorption at certain polarizations and such an orientation seems highly unlikely. A half-ring structure of LH1 oriented perpendicular to the excitation beam can also not explain the polarization behavior as observed in Fig. 5 (type III). In such a case two orthogonal bands will dominate the optical spectrum. A possible explanation is that the type III spectra correspond to a half-ring structure that is tilted with respect to the direction of the excitation beam.

In the type IV spectra two narrow absorption lines are observed (Fig. 5). This indicates the presence of at least two aggregates weakly coupled to each other. There are two possibilities for this kind of behavior. First the spectra might originate in two LH1-RC complexes. Dimerization of the LH1-RC structure was reported by Francia et al. (1999). They proposed a dimeric structure of the LH1-RC complex

under native conditions, which could be converted into a monomeric structure by increasing the detergent concentration during the biochemical isolation. Because our preparation procedure was at a high detergent concentration, a dimeric aggregation of the LH1-RC complexes seems not probable. A second possibility might be the presence of more or less isolated domains of pigment arrays within one LH1 ring. These domains are isolated from each other by either defects in the ring or additional proteins that form part of the LH1 structure but do not participate in the transfer of energy.

CONCLUSIONS

The results presented in this paper show that it is possible to observe the fluorescence-excitation spectra of individual LH1-RC complexes, thus providing for the first time a direct insight into the electronic structure of LH1 at a single-complex level. We conclude that the LH1 assembly of BChl *a* pigments represents a strongly coupled system, similar to that of the B850 ring of LH2. The limited number of bands (3–4) with linewidths of 150 to 200 cm^{-1} and the presence of one or two preferred polarization directions, that were observed for most of the complexes, indicate that the excited states of LH1 at low temperature should be described as collective excitations or Frenkel excitons. The spectra show a large variation in spectral features like the number of bands, bandwidths, and their polarization behavior. Such a variation is not observed for the individual spectra of LH2, which are dominated by site heterogeneity (Ketelaars et al., 2001). We conclude that the structural model proposed for LH2 is only applicable to 30% of the studied LH1 complexes and that other factors come into play when interpreting the spectral features of the remaining complexes. In particular, we suggest that the variation in the optical spectra of individual LH1-RC complexes reflects the heterogeneity in the spatial structure of the LH1 assembly of pigments in combination with various orientations of the complexes in the polymer film, which may be enhanced or even induced by the structural heterogeneity.

It is not clear to what extent these structural variations are representative of LH1-RC complexes in the native system, as they could also be induced by isolation, purification, and deposition of the sample. However, if in the photosynthetic membrane the spatial arrangement of the LH1-RC complexes is in a dynamic equilibrium between complete rings and complexes in the process of being built, the four groups could represent snapshots of different structures. It is believed that the presence of the RC helps to stabilize the LH1 ring in isolated LH1-RC complexes. For example, in comparing the spectra of individual, isolated LH1 rings with those of single LH1-RC complexes, both from *Rps. rubrum*, we observed a much larger spectral variation in the former (M. Ketelaars, unpublished results). It also suggests that the history of the sample might influence the spectral variation of individual complexes.

The experiments presented show that the optical spectra of individual pigment-protein complexes carry valuable information about their spatial structure. Our results represent the first steps in the elucidation of the electronic structure of the LH1 complex at the single-complex level. The results support the view of largely delocalized excited states in the LH1 assembly of pigments. Future advancements may be expected by studying these complexes in a more native-like environment, e.g., through incorporation in lipid bilayers, and by controlling their orientation.

The authors thank Dr. Alastair T. Gardiner (University of Glasgow) for the preparation of the LH1-RC complexes. Substantial financial support from the Volkswagen-Stiftung (Germany, Hannover) is gratefully acknowledged. This work is furthermore part of the research program of the Stichting voor Fundamenteel Onderzoek der Materie (FOM) with financial aid from the Nederlandse Organisatie voor Wetenschappelijk Onderzoek (NWO) and is supported by the Section Earth and Life Sciences (ALW) of the Netherlands Organization for Scientific Research (NWO). M.K. thanks the Center for NanoScience (CeNS) for a grant in the framework of a Marie-Curie Fellowship and the European Molecular Biology Organization (EMBO; project ASTF 9520) for supporting his stay in Munich, where the main part of the experimental work has been performed.

REFERENCES

Alden, R. G., E. Johnson, V. Nagarajan, W. W. Parson, C. J. Law, and R. J. Cogdell. 1997. Calculations of spectroscopic properties of the LH2 bacteriochlorophyll-protein antenna complex from *Rhodopseudomonas acidophila. J. Phys. Chem. B.* 101:4667–4680.

Barz, W. P., F. Francia, G. Venturoli, B. A. Melandri, A. Verméglio, and D. Oesterhelt. 1995a. Role of the PufX protein in photosynthetic growth of *Rhodobacter sphaeroides:* 1. PufX is required for efficient light-driven electron transfer and photophosphorylation under anaerobic conditions. *Biochemistry.* 34:15235–15247.

Barz, W. P., A. Verméglio, F. Francia, G. Venturoli, B. A. Melandri, and D. Oesterhelt. 1995b. Role of the PufX protein in photosynthetic growth of *Rhodobacter sphaeroides:* 2. PufX is required for efficient ubiquinone/ubiquinol exchange between the reaction center Q_b site and the cytochrome bc_1 complex. *Biochemistry.* 34:15248–15258.

Bradforth, S. E., R. Jimenez, F. van Mourik, R. van Grondelle, and G. R. Fleming. 1995. Excitation transfer in the core light-harvesting complex (LH-1) of *Rhodobacter sphaeroides:* an ultrafast fluorescence depolarization and annihilation study. *J. Phys. Chem.* 99:16179–16191.

Cogdell, R. J., P. K. Fyfe, S. J. Barrett, S. M. Prince, A. A. Freer, N. W. Isaacs, P. McGlynn, and C. N. Hunter. 1996. The purple bacterial photosynthetic unit. *Photosynth. Res.* 48:55–63.

Farchaus, J. W., W. P. Barz, H. Grunberg, and D. Oesterhelt. 1992. Studies on the expression of the pufX polypeptide and its requirement for photoheterotrophic growth in *Rhodobacter sphaeroides. EMBO J.* 11: 2779–2788.

Francia, F., J. Wang, G. Venturoli, B. A. Melandri, W. P. Barz, and D. Oesterhelt. 1999. The reaction center-LH1 antenna complex of *Rhodobacter sphaeroides* contains one PufX molecule which is involved in dimerization of this complex. *Biochemistry.* 38:6834–6845.

Francke, C., and J. Amesz. 1995. The size of the photosynthetic unit in purple bacteria. *Photosynth. Res.* 46:347–352.

Freiberg, A. 1995. Coupling of Antennas to Reaction Centers. *In* Anoxygenic Photosynthetic Bacteria. R. E. Blankenship, M. T. Madigan, and C. E. Bauer, editors. Kluwer Academic Publishers, Dordrecht. 385–398.

Frese, R. N., J. D. Olsen, R. Branvall, W. H. J. Westerhuis, C. N. Hunter, and R. van Grondelle. 2000. The long-range supraorganization of the bacterial photosynthetic unit: a key role for PufX. *Proc. Natl. Acad. Sci. U.S.A.* 97:5197–5202.

Gall, A. 1995. Purification, characterisation and crystallisation from a range of *Rhospirillineae* pigment-protein complexes. Thesis, University of Glasgow, U.K.

Ghosh, R., S. Ghosh-Eicher, M. DiBerardino, and R. Bachofen. 1994. Protein phosphorylation in *Rhodospirillum:* purification and characterization of a water-soluble B873 protein kinas and a new component of the B873 complex, Ω, which can be phosphorylated. *Biochim. Biophys. Acta.* 1184:28–36.

Ghosh, R., A. Hoenger, D. Mihailescu, R. Bachofen, A. Engel, and J. P. Rosenbusch. 1994. Two-dimensional crystallization of the light-harvesting complex from *Rhodospirillum rubrum. J. Mol. Biol.* 231: 501–504.

Hawthornthwaite, A. M., and R. J. Cogdell. 1991. Bacteriochlorophyll binding proteins. *In* Chlorophylls. H. Scheer, editor. CRC Press, Boca Raton, FL. 493–528.

Hu, X., T. Ritz, A. Damjanovic, and K. Schulten. 1997. Pigment organization and transfer of electronic excitation in the photosynthetic unit of purple bacteria. *J. Phys. Chem. B.* 101:3854–3871.

Jimenez, R., F. van Mourik, J. Y. Yu, and G. R. Fleming. 1997. Three-pulse photon echo measurment on LH1 and LH2 complexes of *Rhodobacter sphaeroides:* a nonlinear spectroscopic probe of energy transfer. *J. Phys. Chem. B.* 101:7350–7359.

Jungas, C., J.-L. Ranck, J.-L. Rigaud, P. Joliot, and A. Verméglio. 1999. Supramolecular organization of the photosynthetic apparatus of *Rhodobacter sphaeroides. EMBO J.* 18:534–543.

Karrasch, S., P. A. Bullough, and R. Ghosh. 1995. The 8.5 angstrom projection map of the light-harvesting complex I from *Rhodospirillum rubrum* reveals a ring composed of 16 subunits. *EMBO J.* 14:631–638.

Ketelaars, M., A. M. van Oijen, M. Matsushita, J. Köhler, J. Schmidt, and T. J. Aartsma. 2001. Spectroscopy of the B850 band of individual light-harvesting 2 complexes of *Rhodopseudomonas acidophila:* I. Experiments and Monte-Carlo simulations. *Biophys. J.* 80:1591–1603.

Koepke, J., X. C. Hu, C. Muenke, K. Schulten, and H. Michel. 1996. The crystal structure of the light-harvesting complex II (B800–850) from *Rhodospirillum molischianum. Structure.* 4:581–597.

Law, C. J. 1998. Thesis, University of Glasgow, U.K.

Lilburn, T. G., C. E. Haith, S. Prince, and J. T. Beatty. 1992. Pleiotropic effects of *pufX* gene deletion on the structure and function ofthe photosynthetic apparatus of *Rhodobacter capsulatus. Biochim. Biophys. Acta.* 110:160–170.

Matsushita, M., M. Ketelaars, A. M. van Oijen, J. Köhler, T. J. Aartsma, and J. Schmidt. 2001. Spectroscopy on the B50 band of individual light-harvesting 2 complexes of *Rhodopseudomonas acidophila:* II. Exciton states of an elliptically deformed ring aggregate. *Biophys. J.* 80:1604–1614.

McDermott, G., S. M. Prince, A. A. Freer, A. M. Hawthomthwaite-Lawless, M. Z. Papiz, R. J. Cogdell, and N. W. Isaacs. 1995. Crystal structure of an integral membrane light-harvesting complex from photosynthetic bacteria. *Nature.* 374:517–521.

McGlynn, P., C. N. Hunter, and M. R. Jones. 1994. The *Rhodobacter sphaeroides* PufX protein is not required for photosynthetic competence in the absence of a light harvesting system. *FEBS Lett.* 349:517–521.

McGlynn, P., W. H. Westerhuis, M. R. Jones, and C. N. Hunter. 1996. Consequences for the organization of reaction center-light harvesting antenna 1 (LH1) core complexes of *Rhodobacter sphaeroides* arising from the deletion of amino acid residues from the C terminus of the LH1 polypeptide. *J. Biol. Chem.* 271:3285–3292.

McLuskey, K., S. M. Prince, R. J. Cogdell, and N. W. Isaacs. 2001. The crystallographic structure of the B800–820 LH3 light-harvesting complex from the purple bacteria *Rhodopseudomonas acidophila* strain 7050. *Biochemistry.* 40:8783–8789.

Meckenstock, R. U., K. Krusche, R. A. Brunisholz, and H. Zuber. 1992. The light-harvesting core-complex and the B820-subunit from *Rhodopseudomonas marina:* Part II. Electron microscopic characterisation. *FEBS Lett.* 311:135–138.

Mostovoy, M. V., and J. Knoester. 2000. Statistics of optical spectra from single ring-aggregates and its application to LH2. *J. Phys. Chem. B.* 104:12355–12364.

Novoderezhkin, V. I., and A. P. Razjivin. 1994. Exciton states of the antenna and energy trapping by the reaction center. *Photosynth. Res.* 42:9–15.

Novoderezhkin, V. I., and A. P. Razjivin. 1995. Exciton dynamics in circular aggregates: apllication to antenna of photosynthetic purple bacteria. *Biophys. J.* 68:1089–1100.

Papiz, M. Z., S. M. Prince, A. M. Hawthornthwaite-Lawless, G. McDermott, A. A. Freer, N. W. Isaacs, and R. J. Cogdell. 1996. A model for the photosynthetic apparatus of purple bacteria. *Trends Plant Sci.* 1:198–206.

Parkes-Loach, P. S., C. J. Law, P. A. Recchia, J. W. Kehoe, S. Nehrlich, J. Chen, and P. A. Loach. 2001. Role of the core region of the PufX protein in inhibition of reconstitution of the core light-harvesting complexes of *Rhodobacter sphaeroides* and *Rhodobacter capsulatus. Biochemistry.* 40:5593–5601.

Pearlstein, R. M. 1991. Theoretical interpretation of antenna spectra. *In* Chlorophylls. H. Scheer, editor. CRC Press, Boca Raton, FL. 1047–1078.

Qians, P., T. Agura, Y. Oyama, and R. J. Cogdell. 2000. Isolation and purification of the reaction center (RC) and the core (RC-LH1) complex from *Rhodobium marinum:* the LH1 ring of the detergent-solubilized core complex contains 32 bacteriochlorophylls. *Plant Cell Physiol.* 41:1347–1353.

Recchia, P. A., C. M. Davis, T. G. Lilburn, J. T. Beatty, P. S. Parkes-Loach, C. N. Hunter, and P. A. Loach. 1998. Isolation of the PufX protein from *Rhodobacter* capsulatus and *Rhodobacter sphaeroides:* evidence for its interaction with the alpha-polypeptide of the core light-harvesting complex. *Biochemistry.* 37:11055–11063.

Reddy, N. R. S., R. Picorel, and G. J. Small. 1992. B896 and B870 components of the *Rhodobacter sphaeroides* antenna: a hole burning study. *J. Phys. Chem.* 96:6458–6464.

Rijgersberg, C. P., R. van Grondelle, and J. Amesz. 1980. Energy transfer and bacteriachlorophyll fluorescence in purple bacteria at low temperature. *Biochim. Biophys. Acta.* 592:53–64.

Sauer, K., R. J. Cogdell, S. M. Prince, A. A. Freer, N. W. Isaacs, and H. Scheer. 1996. Structure-based calculations of the optical spectra of the LH2 bacteriochlorophyll-protein complex from *Rhodopseudomonas acidophila. Photochem. Photobiol.* 64:564–576.

Somsen, O. J. G., F. van Mourik, R. van Grondelle, and L. Valkunas. 1994. Energy migration and trapping in a spectrally and spatially inhomogenous light-harvesting antenna. *Biophys. J.* 66:1580–1596.

Stahlberg, H., J. Dubochet, H. Vogel, and R. Ghosh. 1998. The reaction centre of the photounit of *Rhodospirillum rubrum* is anchored to the light-harvesting complex with four-fold rotational disorder. *Photosynth. Res.* 55:363–368.

Stark, W., W. Kühlbrandt, I. Wildhaber, E. Wehrli, and K. Muhlethaler. 1984. The structure of the photoreceptor unit of *Rhodobacter viridis. EMBO J.* 3:777–783.

Sundström, V., and R. van Grondelle. 1995. Kinetics of excitation transfer and trapping in purple bacteria. *In* Anoxygenic Photosynthetic Bacteria. R. E. Blankenship, M. T. Madigan, and C. E. Bauer, editors. Kluwer Academic Publishers, Dordrecht. 349–372.

Valkunas, L., F. van Mourik, and R. van Grondelle. 1992. On the role of spectral and spatial antenna inhomogeneity in the process of excitation energy trapping in photosynthesis. *J. Photochem. Photobiol. B.* 15: 159–170.

van Amerongen, H., L. Valkunas, and R. van Grondelle. 2000. Photosynthetic excitons. Worldzsn Scientific, Singapore.

van Mourik, F., R. W. Visschers, and R. van Grondelle. 1992. Energy transfer and aggregate size effects in the inhomogenously broadened core light-harvesting complex of *Rhodobacter sphaeroides. Chem. Phys. Lett.* 193:1–7.

van Oijen, A. M., M. Ketelaars, J. Köhler, T. J. Aartsma, and J. Schmidt. 1998. Spectroscopy of single light-harvesting complexes from purple photosynthetic bacteria at 1.2 K. *J. Phys. Chem. B.* 102:9363–9366.

van Oijen, A. M., M. Ketelaars, J. Köhler, T. J. Aartsma, and J. Schmidt. 1999a. Unraveling the electronic structure of individual photosynthetic pigment-protein complexes. *Science.* 285:400–402.

van Oijen, A. M., M. Ketelaars, J. Köhler, T. J. Aartsma, and J. Schmidt. 1999b. Spectroscopy of individual LH2 complexes of *Rhodopseudomonas acidophila:* localized excitations in the B800 band. *Chem. Phys.* 247:53–60.

van Oijen, A. M., M. Ketelaars, J. Köhler, T. J. Aartsma, and J. Schmidt. 2000. Spectroscopy of individual LH2 complexes of *Rhodopseudomonas acidophila:* diagonal disorder, intercomplex heterogeneity, spectral diffusion, and energy transfer in the B800. *Biophys. J.* 78:1570–1577.

Visschers, R. W., C. Chang, F. van Mourik, P. S. Parkes-Loach, B. A. Heller, P. A. Loach, and R. van Grondelle. 1991. Fluorescence polarization and low-temperature absorption spectroscopy of a subunit form of light-harvesting complex I from purple photosynthetic bacteria. *Biochemistry.* 30:5734–5742.

Visser, H. M., O. J. G. Somsen, F. van Mourik, I. H. M. van Stokkum, and R. van Grondelle. 1995. Direct observation of sub-picosecond equilibration of excitation energy in the light-harvesting antenna of *Rhodospirillum rubrum. Biophys. J.* 69:1083–1099.

Walz, T., S. J. Jamieson, C. M. Bowers, P. A. Bullough, and C. N. Hunter. 1998. Projection structures of three photosynthetic complexes from *Rhodobacter sphaeroides:* LH2 at 6 angstrom LH1 and RC-LH1 at 25 angstrom. *J. Mol. Biol.* 282:833–845.

Westerhuis, W. H. J., C. N. Hunter, R. van Grondelle, and R. A. Niederman. 1999. Modeling of oligomeric-state dependent spectral heterogeneity in the B875 light-harvesting complex of *Rhodobacter sphaeroides* by numerical simulation. *J. Phys. Chem. B.* 103:7733–7742.

Wu, H.-M., M. Ratsep, R. Jankowiak, R. J. Cogdell, and G. J. Small. 1997. Comparison of the LH2 antenna complexes of *Rhodopseudomonas acidophila* (strain 10050) and *Rhodobacter sphaeroides* by high-pressure absorption, high-pressure hole burning, and temperature-dependent absorption spectroscopies. *J. Phys. Chem. B.* 101:7641–7653.

Wu, H.-M., M. Ratsep, R. Jankowiak, R. J. Cogdell, and G. J. Small. 1998. Hole-burning and absorption studies of the LH1 antenna complex of purple bacteria: effects of pressure and temperature. *J. Phys. Chem. B.* 102:4023–4034.

Wu, H.-M., and G. J. Small. 1997. Symmetry adapted basis defect pattern for analysis of the effects of energy disorder on cyclic arrays of coupled chromophores. *Chem. Phys.* 218:225–234.

Yeates, T. O., H. Komiya, A. Chirino, D. C. Rees, J. P. Allen, and G. Feher. 1988. Structure of the raction center from *Rhodobacter sphaeroides* R-26 and 2.4.1: protein cofactor (bacteriochlorophyll, bacteriopheophytin and carotenoid) interactions. *Proc. Natl. Acad. Sci. U.S.A.* 85:7993–7997.

Zuber, H., and R. J. Cogdell. 1995. Stucture and organization of purple bacteria antenna complexes. *In* Anoxygenic Photosynthetic Bacteria. R. E. Blankenship, M. T. Madigan, and C. E. Bauer, editors. Kluwer Academic Publishers, Dordrecht. 315–348.